Development of an Apparatus for Biaxial Testing Using Cruciform Specimens

by A. Makinde, L. Thibodeau and K.W. Neale

ABSTRACT—A testing apparatus has been developed to study the behavior of sheet metals and composite materials under monotonic and cyclic biaxial loading conditions. This test facility employs cruciform specimens that are loaded in their plane. Problems encountered while developing the test system are discussed.

We also discuss the difficulties common to test methods employing cruciform specimens. These relate to the design of a suitable specimen geometry and to the determination of the stresses throughout the specimen. A method for designing an optimal geometry for these specimens is presented. This method is based on the statistical tools of factorial and response surface designs. The statistical method, coupled with a finite-element analysis of the specimen, was successfully applied to optimize the geometry of a cruciform specimen with a circular reduced central region.

Introduction

The ability to successfully model and simulate the behavior of materials, for optimum use in structural applications and in metal forming operations, depends largely on the material description (constitutive relations, yield and failure criteria) employed in the analytical formulation. Recent advances in computer technology have resulted in a reduction in computing costs such that complex analyses can now be carried out. The main difficulty which remains at present concerns the proper choice of constitutive law. Rigorous experimental characterization is necessary for this purpose in order to ensure that the constitutive model adequately describes the behavior of the material under a variety of complex loading conditions. Biaxial experiments are needed to approximate as much as possible the conditions that sheet materials may be subjected to in practice. These tests are also necessary to quantify and clarify the effects of stress biaxiality on: monotonic and cyclic stress-strain curves, fatigue crack initiation and propagation, and forming limit diagrams. Furthermore, a critical comparison of predictions of a material model with experimental results may suggest directions for further improvement in constitutive laws. Such complex experiments demand expensive and sophisticated test equipment and procedures.

A. Makinde (SEM Member) is Research Associate, L. Thibodeau is Technician, and K.W. Neale is Professor, Université de Sherbrooke, 2500, boul. Université, Sherbrooke, Québec, J1K 2R1, Canada.

Paper was presented at the 1989 SEM Spring Conference on Experimental Mechanics held in Cambridge, MA on May 28-June 8.

Original manuscript submitted: October 7, 1991. Final manuscript received: February 5, 1992.

Different techniques have been developed for producing biaxial stress states in materials. These vary in design and complexity depending on the geometry of the specimen employed. The most common method of biaxial testing employs thin-walled circular tubes subjected to a variety of loads: axial, torsional and internal/external pressure.[1,2] These loads can be applied independently or simultaneously. The technique is very versatile and allows for all possible biaxial stress states to be imposed on the tube.[2] However, it is not suitable for large strain studies of anisotropic materials. This is because of buckling and necking instabilities which may arise before very large strains are attained. Also, radial stress gradients may not be negligible depending on the thickness of the tube and the applied loads. Furthermore, tubular specimens are not suitable for rolled sheet or for laminated composite materials.

The most appropriate method for testing sheet materials consists of applying in-plane biaxial loads to cruciform specimens. Various techniques are in use for the application of the loads. These can be classified according to the load-frame configuration and the method of application of the mutually orthogonal loads. The load reaction can be either 'in-plane' or 'out-of-plane'. For in-plane frame configurations the load frame surrounds the specimen,[3-13] while for out-of-plane systems it is on one side of the specimen.[14-18] Out-of-plane frames are subject to bending moments under load and must be extremely stiff to reduce the deflection normal to the plane of the frame to a minimum. Different techniques are also employed in the design of the load train. For biaxial creep testing, out-of-plane deadweight loading systems with hinged levers have been employed.[14-16] For monotonic tensile testing, in-plane biaxial displacement devices that are mounted directly onto a conventional uniaxial testing machine have been proposed. These include a bidirectional cable and pulley system proposed by Bert *et al.*[12] and an inexpensive spatial pantograph recently proposed by Ferron and Makinde.[13] However, with these devices, the loading axes are not independent of each other and, consequently, the possible biaxial strain paths are very limited.

The most versatile method for testing cruciform specimens under monotonic and cyclic loading conditions consists in using servohydraulic actuators to apply the loads. Different designs of actuator-based systems have also been proposed. In-plane frame designs with two, three and four actuators have been proposed.[3-11] Out-of-plane frame designs with two and four actuators are also in use.[17,18] Systems with less than four actuators subject

the specimen to side bending loads, irrespective of the load-frame configuration. Also, the center of the specimen is never stationary during testing with such systems.

In this paper we describe a biaxial testing apparatus recently developed at the Université de Sherbrooke.[19] This apparatus employs four servohydraulic actuators for testing cruciform specimens under monotonic and cyclic loading conditions. We also carry out a finite-element study of the specimen shape leading to the proposal of an optimized geometry.

Description of the Biaxial Testing Apparatus

The apparatus is comprised of three major groups of elements: the loading system, the control system, and the specimen.

Loading System

The loading system consists of the load reaction frame and the load train. In the initial design stage of the load frame, an octagonal in-plane frame similar to the one proposed by Pascoe *et al.*[3,4] was considered. However, it was found that, for the frame to be sufficiently rigid, it had to be very large and would be expensive to construct. The design that was finally chosen is an out-of-plane configuration as depicted in Fig. 1. The reasons that motivated this choice were: cost, ease of manufacture and assembly. Because the frame is subjected to high bending stresses under load, it was massively constructed to reduce to a minimum any extraneous forces on the specimen. Frame rigidity was assured by using a cross-shaped steel slab about 152-mm thick and an I-beam welded to the underside of the steel slab (Fig. 1). Under the most unfavorable loading condition, that is, maximum compressive loads along the two axes, the maximum deflection is less than 0.1 mm at the center of the frame.

Along each loading axis are two linear hydraulic actuators (MTS Model 244.31) of a rated capacity of 250 kN. Each actuator is mounted on a rigid block that is, in turn, firmly bolted to the steel slab and I-beam assembly, as shown in Fig. 1. Two actuators are employed per loading axis to eliminate any movement of the center of the specimen during testing. Opposing actuators are connected to common hydraulic lines so that they exert an equal but opposite force on each other. A load cell is included in each loading direction. Hydraulic wedge grips, designed and manufactured in our workshop, complete the load trains. These grips are preloaded and hydraulically locked prior to starting a test. The components of the load trains are connected together by threaded studs. To provide a backlash-free connection under cyclic loading, preloaded spiral washers[20] are employed over the connecting studs to remove any slack that may be present in the load train.

Control System

Two electrohydraulic closed-loop channels independently control the two axes of the machine. The control system is comprised of two servocontrollers, a hydraulic distribution system, and force, displacement and strain control circuits. A schematic of the control loop for a typical loading axis is presented in Fig. 2. Each electrohydraulic channel is controlled by a microprocessor-based servocontroller (MTS Model 458.20 Microconsole). Input command signals to the servocontroller are produced by two digital function generators that provide unlimited possibilities with regard to waveform shape. Different waveforms as well as out-of-phase signals can be used along the loading directions. The function generator is capable of frequencies in the range 0.00001-990 Hz and ±10-V signal amplitudes. For dynamic reasons, however, the load frame limits the maximum frequency to 35 Hz at maximum load levels along the two axes. During a test the servocontrollers transmit command signals from the function generators to the servovalves and compare the command signals with the feedback signals measured by the load, displacement or strain transducers depending on the parameter being used to control the test.

The hydraulic system consists of servovalves, pressure accumulators, manifolds and a 265-ℓ/min, 21-MPa hydraulic pump. The hydraulic fluid is pumped in closed circuit through a 3-micron filter and an air-cooled heat-exchanger to maintain its temperature constant. The servovalves regulate the flow of hydraulic fluid into the actuators and provide closed-loop control.

Each actuator is equipped with a linear-variable differential transformer (LVDT) that is used to control the actuators during the setup and completion phases of a test. The displacement range per actuator is from 0 to 152 mm. During a test, the LVDT measures the displacement of each actuator piston rod and the outputs of the pair along a loading direction can be compared to ensure that the center of the specimen remains fixed. Also, the LVDTs can serve as feedback inputs to the servocontroller for displacement control with a possible range of ±152 mm per loading axis.

Apart from the possibility of actuator-piston displacement control, two other control modes are possible:

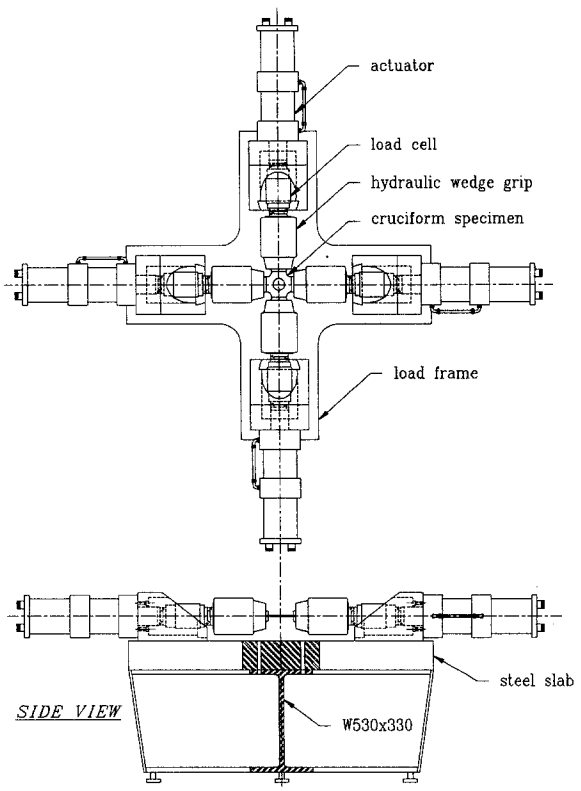

Fig. 1—Plan and side views of the biaxial testing apparatus

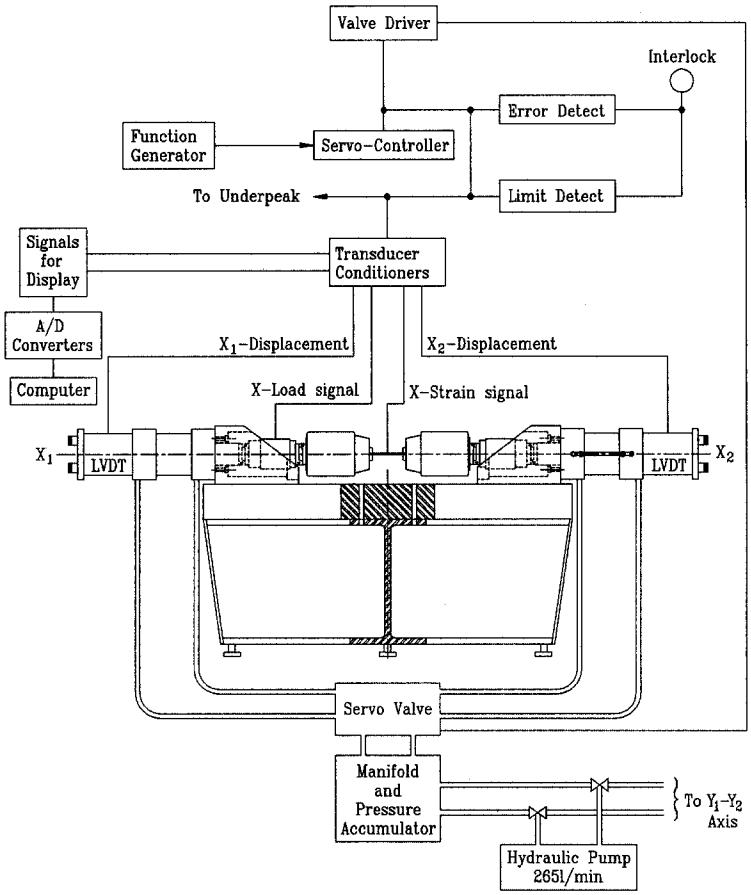

Fig. 2—Hydraulic and control circuits for a typical axis of the biaxial testing apparatus

force (±250 kN) and strain. The strain range depends on the type of test and specimen design. To utilize the strain-control mode, a specially designed extensometer is employed. This extensometer provides independent measurements of strains along two mutually perpendicular directions. Details concerning this original extensometer are provided in a companion article by Makinde *et al.*[21]

The two servocontrollers are interfaced to a personal computer for digital data acquisition. Measurements from load cells, LVDTs and strain transducers are transmitted to the personal computer through 14-bit analog/digital converters that allow simultaneous readings of all transducer outputs. A photograph of the test apparatus is shown in Fig. 3.

Specimen Geometry

An important element in any test system design is the specimen design. The specimen geometry, the manner in which stresses are calculated from applied loads and the uniformity of stress and strain fields in the gage section all greatly influence the test results and their interpretation. For this test facility, we employ cruciform specimens for which there is not yet any standardized geometry. This lack of a standard geometry has meant so far that correlations of results from different laboratories are often difficult. For example, a literature review by Smith and Pascoe[22] of fatigue-crack-propagation studies by different workers employing cruciform specimens showed conflicting evidence on the behavior of cracks subject to biaxial stress fields. Two different specimen geometries are generally employed in biaxial tests. For tests involving small strains (e.g., fatigue crack initiation and propagation, composite-materials testing) cruciform specimens with a reduced circular central section have generally been used. A typical example of this geometry is shown in Fig. 4(a). For large strain studies on the other hand, cruciform specimens having a rectangular central section with slots in the arms, as depicted in Fig. 4(b), are usually employed. These slots are employed to reduce the rigidity of the arms which might otherwise restrict the maximum strain attainable in the center of the specimen and the size of the region of homogeneous stress and strain fields.[23]

Aside from the lack of a standard design for these specimens, other problems are encountered in their use.

Fig. 3—Photograph of the biaxial testing apparatus

The most important problem deals with stress concentrations at the corner fillets and in the transition zone, that is the zone of change in thickness from the arms to the test section. For specimens with slotted arms [Fig. 4(b)] the roots of the slots, especially those near the test area, also constitute sources of unavoidable stress concentrations. These high stress-concentration areas usually lead to a premature failure of the specimen. The means of overcoming them have proved so far difficult to accomplish in practice.

Another problem associated with the use of cruciform specimens relates to the manner of calculating stresses from the loads applied on the arms of the specimen. This also varies from laboratory to laboratory. Some use finite-element analyses which may be appropriate under linear-elastic loading.[24] For elasto- or viscoplastic behavior, however, the need to use a constitutive relation in the finite-element analysis mitigates the usefulness of such results. Others use experimentally determined strain values[6,12,25] while some define effective cross-sectional areas that depend on load or biaxial strain ratio.[26] Others use the cross-sectional area of the center of the specimen.[16,27] without regard to the part of the loads carried by the corner fillets, and still some simply use the cross-sectional area of the arms.[28] We are currently developing a method based on the definition of effective cross-sectional areas calculated from experimentally determined strain values. This method will be presented in a subsequent paper.

Optimization of the Geometry of Cruciform Specimens

It is clear from the above discussions that many factors influence the accuracy of test results from cruciform specimens. To reduce the influence of the specimen geometry on our test results, we have undertaken a study of the factors that may influence the stress and strain distributions and the failure or limit strains in the specimens.

The number of geometrical factors that may influence the stress/strain distribution and the limit strains in a cruciform specimen vary considerably, depending on the geometry. For the geometry shown in Fig. 4(a), that is used for low-strain studies, there are at least seven geometrical variables assuming a perfectly machined specimen. These seven variables are: (1) width of the arms: $2W_a$, (2) length of the specimen *outside* the grips: $2L$, (3) corner fillet radius between the arms: R_f, (4) radius of the circular central region: R_c, (5) radius of transition: R_t, (6) thickness of the arms: T_a, (7) ratio of thickness of the arm to the thickness of the gage section: T_a/T_g.

For the slotted cruciform specimen shown in Fig. 4(b), there are potentially five other geometrical factors besides the seven mentioned above: (a) width of the central section: $2W_c$ (note $W_c > R_c$ in this case), (9) diameter of slots: Dslot, (10) number of slots: Nslot, (11) length of slots: Lslot and, (12) positions of the slots: Xslot(i), $i = 1$, Nslot.

The question that arises is how to determine an optimal combination of the variables that meets the required objectives for each type of geometry, the objectives being uniform stress and strain distributions in the specimen for both geometries and, in addition, a high limit strain for the slotted geometry. The traditional way of changing one variable at a time may not lead to an optimal design because of the possibility of interactions between two or more of the variables.

A statistical design and analysis of the combinations of the variables to be studied was adopted here. Details on

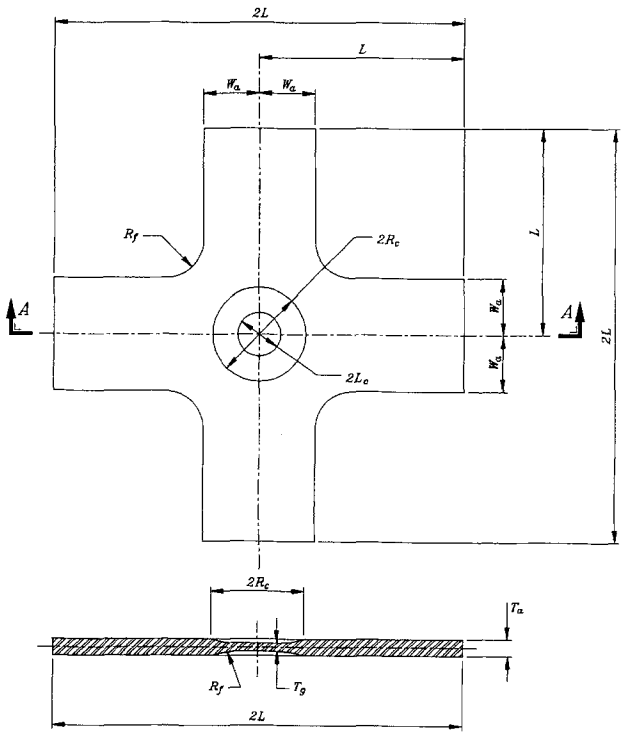

SECTION A–A

Fig. 4(a)—Typical cruciform specimen with a circular reduced central section

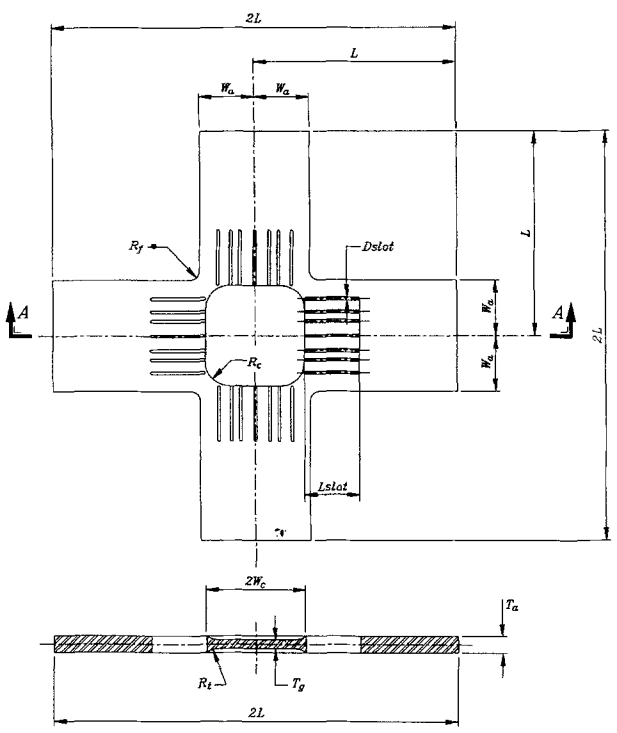

SECTION A–A

Fig. 4(b)—Typical cruciform specimen with slots on the arms

the application of the factorial design technique will be presented elsewhere. Specifically, two levels of each variable were studied using factorial, fractional factorial and response surface designs.[29] For each combination of the variables, the measured effects were: the widths of the zones over which the stresses and the strains are uniform to within five percent in the center of the specimen, and the limit strains. The limit strain was defined as the maximum strain attained in the center of the specimen prior to failure. In the statistical design, it is necessary to introduce initial upper and lower levels for each geometrical factor. For the specimen with the circular center, two different geometries that were the results of elastic finite-element modeling have been proposed by Liu *et al.*[24] and Wilson and White.[30] Table 1 shows the different values of the variables proposed by the two groups of researchers. The uniformity of the strain field in the specimen proposed by Wilson and White[30] was, in addition, ascertained through photoelastic studies. The initial lower and upper levels of the geometrical factors were chosen according to Table 1 for the present study.

The statistical analysis and design technique was applied to optimize only the geometry of the specimen with a circular reduced center in the present study. To study the effects of the variables on the different geometries resulting from the factorial designs, we have undertaken an elasto-plastic finite-element analysis of the specimen. The statistical experiments are then a collection of runs of the finite-element model. For the specimen with a circular central region, we are primarily concerned with the uniformity of stress and strain fields within the gage length.

Finite-element Analysis

The finite-element method is adopted to formulate a computational scheme for the evaluation of the stress and strain distributions in the cruciform specimen. The governing relations used in the formulation of the problem are derived from Hill's[31] general theory for statically deformed solids at finite strains and discussed by Hutchinson[32] for a Lagrangian formulation. The stress across the thickness of the material is assumed uniform and the above formulation is specialized to generalized plane-stress conditions.

The finite-element equations were developed using an extremum principle due to Hill.[31] This principle states that the incremental equilibrium behavior of the solid is governed by the following variational equation.

$$\delta \left(\int_{V_0} \frac{1}{2} \left(L^{ijkl} \dot{\eta}_{ij} \dot{\eta}_{kl} + \tau^{ij} \dot{u}^k_{,i} \dot{u}_{k,j} \right) dV_0 - \int_{S_T} \dot{T}^i \dot{u}_i dS \right) = 0 \qquad (1)$$

Here S_T represents the part of the surface on which nominal traction increments $\dot{\mathbf{T}}$ are prescribed, L^{ijkl} denotes the tensor of instantaneous moduli, τ^{ij} is the Kirchhoff stress tensor and $\dot{\eta}_{ij}$ are the Lagrangian strain-rate components. The u_i and u^i denote, respectively, the covariant and contravariant components of the displacement vector and a comma represents covariant differentiation with respect to the undeformed metric. The specific form of the instantaneous moduli L^{ijkl} depends on the plasticity theory adopted. In this study, the isotropic hardening J_2 flow theory of plasticity is employed.[32,33]

The uniaxial stress-natural strain curve adopted in this study is the following power-law relationship:

$$\frac{\sigma}{\sigma_y} = \begin{cases} \dfrac{E}{\sigma_y} \epsilon & \text{if } \sigma \le \sigma_y \\ \left(\dfrac{E}{\sigma_y} \epsilon \right)^N & \text{if } \sigma \ge \sigma_y \end{cases} \qquad (2)$$

Here σ_y is the uniaxial yield stress, E is the elastic modulus and N is the work-hardening exponent. The analyses are carried out for $\sigma_y/E = 0.0018$ and $N = 0.22$, values typical of a mild steel.

Figure 5 shows a typical discretization of the specimen into quadrilateral elements. The origin of the radial fan in the discretization is offset from the center of the specimen to ensure that the Gaussian points of the elements along the axes are equidistant from the central axes of the specimen. This facilitates the determination of the variations of the stresses and strains along the specimen axes. Each quadrilateral element was further divided by the diagonals into four constant strain triangles. Because of symmetry, only a quarter of the specimen is analyzed. The boundary conditions are also depicted in Fig. 5. Details of the finite-element analysis are as described by Neglo *et al.*[33]

Optimum Specimen Geometry

The results of the finite-element analysis and the statistical analysis lead to the following values of the optimum geometrical parameters for metal alloys:

$$L \ge 2W_a$$

$$R_f = \frac{2}{3} W_a$$

$$R_c = \frac{23}{25} W_a$$

$$R_t = \frac{4}{3} W_a$$

$$4 \le T_a/T_g \le 6$$

The maximum dimension for the width of the arms ($2W_a$) can be chosen according to the capacity of the testing machine. Limits on the thickness of the arms T_a depend on the material being tested and must be chosen to ensure that plane-stress conditions remain valid.

Figures 6(a) and (b) give the results of the finite-element analyses of the specimen geometry proposed in this study and those proposed by Liu *et al.*[24] and Wilson and White[30] (Table 1). For each of the three geometries, the imposed displacement rates $\dot{u} = \dot{v} = 0.001$ mm per iteration. The iterations were carried out until a total strain value $\epsilon_1 = 0.003$ was reached at the center of the specimen. This strain level corresponds to a plastic strain $\epsilon_1^p = 0.002$. In Figs. 6(a) and (b), L_o represents the length of the gage section and x is the distance along the x axis from the center of the specimen. The figures compare the

TABLE 1—DIMENSIONS OF CRUCIFORM SPECIMENS WITH CIRCULAR REDUCED CENTRAL SECTION PROPOSED BY LIU *ET AL.*[24] AND WILSON AND WHITE[30]

Authors	W_a (mm)	L/W_a	R_f/W_a	R_c/W_a	R_t/W_a	T_a (mm)	T_a/T_g
Liu *et al.*[24]	88.90	2.5714	0.5714	1.4286	3.5943	12.700	2.7778
Wilson and White[30]	31.75	5.0000	1.5000	1.5720	2.7360	15.875	6.2500

strain and stress gradients inside the gage length for the three geometries. It can be seen from Fig. 6(a) that the strains are uniform, to a maximum deviation of five percent over at least 50 percent of the gage section for all the geometries. However, the geometry proposed in this study produces the most uniform strain distribution. The comparison of the stress gradients presented in Fig. 6(b) show that the stress distributions are practically uniform over the gage lengths of the specimen proposed in this study and that by Wilson and White.[30]

Discussion

During the development of the biaxial testing apparatus various obstacles were encountered. These dealt mainly with the alignment of the load trains and with ensuring that the center of the specimen remains fixed during testing. The alignment problem was easily solved through very careful remachining of the individual components of the load trains. The problem of the displacement of the center of the specimen was due mainly to the design of the hydraulic circuit (Fig. 2). Although it was thought that having the same pressure difference in opposing pairs of actuators would lead to the same force, it was discovered that this depended very much on the position of the servovalve with respect to the two opposing actuators. The solution finally adopted consisted in modifying the hydraulic circuit of Fig. 2 and using a servovalve and a pressure accumulator per actuator.

A number of tests are currently being conducted with the biaxial apparatus to characterize the strength of fiber-reinforced composite laminae and to study the behavior of metal alloys under biaxial loading. The tests on the composite laminae have not yet been entirely successful because failure in the center of the specimen is difficult to achieve. This is due in part to fabrication problems. We are currently examining the numerical optimization of the geometry of these specimens. A number of pilot tests on cruciform metal specimens loaded biaxially have been successful. Typical load-elongation curves obtained under equibiaxial loading are shown in Fig. 7 for commercially pure aluminum specimens machined in our laboratory. Figure 8 shows typical force-strain hysteresis curves obtained under cyclic loading on A516 Grade 70 steel using the specimen proposed in this study. In these tests, the strains in the center of the specimen were controlled using the specially designed biaxial extensometer presented in a companion article.[21]

Conclusion

A biaxial testing apparatus has been developed for testing metals and composite materials in sheet form under biaxial loading. The factors which presently limit the full use of the test facility are the lack of standard and suitable cruciform specimen design. This aspect is now being addressed through finite-element modeling.

A method for identifying and optimizing the important variables in a computer model is presented. This method employs the statistical tools of factorial and response

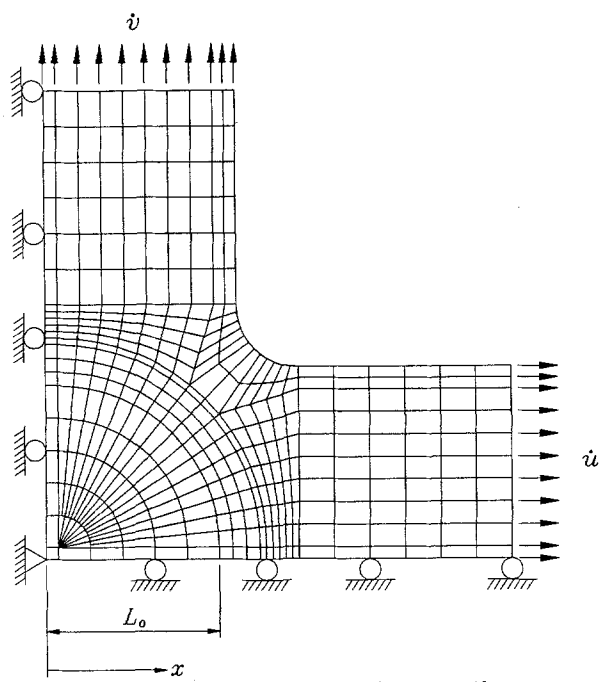

Fig. 5—Discretization of a quarter of the cruciform specimen with a circular reduced central section

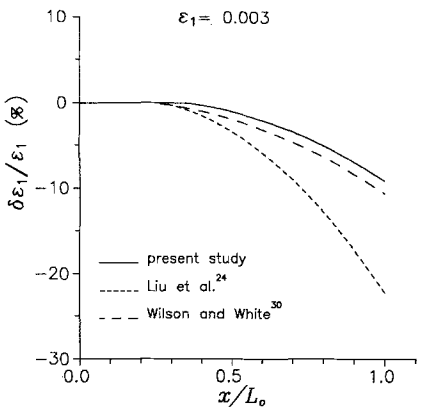

Fig. 6(a)—Estimation of the degree of nonuniformity of strain inside the gage length for three cruciform specimens

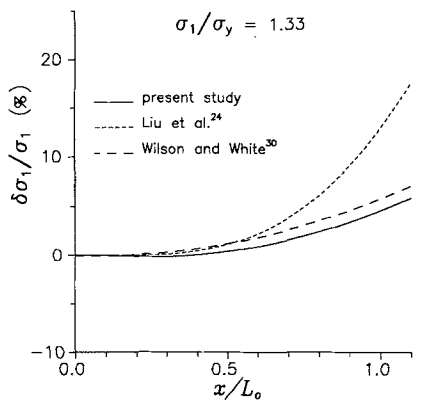

Fig. 6(b)—Estimation of the degree of nonuniformity of stress inside the gage length for three cruciform specimens

surface designs. An example of an optimal cruciform specimen arrived at through the statistical process is presented. The stress and strain distributions in the optimized specimen geometry are found to be excellent in comparison to other geometries that have been proposed in the literature. Work is still progressing on the design of an optimal geometry for large strain studies on metal alloys.

Acknowledgments

This work was supported by the Natural Sciences and Engineering Research Council of Canada and the Government of the Province of Quebec (Programme FCAR).

References

1. Lefebvre, D., Chebl, C., Thibodeau, L. and Khazzari, E., "A High-Strain Biaxial-Testing Rig for Thin-Walled Tubes Under Axial Load and Pressure," EXPERIMENTAL MECHANICS, **23**, *384-392 (1983).*

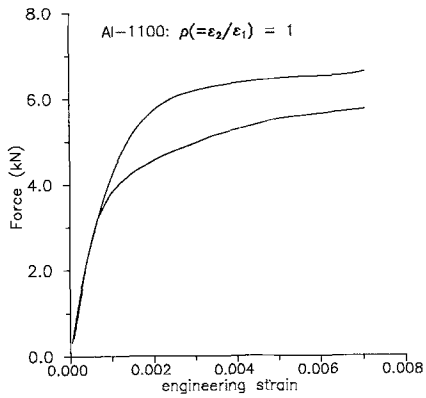

Fig. 7—Force versus engineering strain for commercially pure aluminum Al-1100 under equilibrium loading

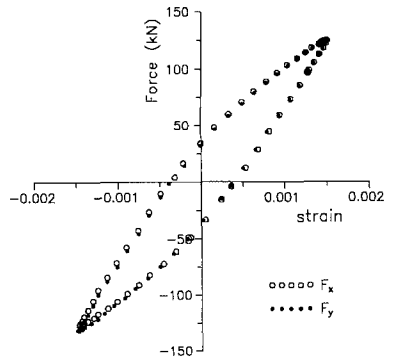

Fig. 8—Force versus strain hysteresis curves for A516-grade 70 steel under equibiaxial cyclic loading

2. Found, M.S., Fernando, U.S. and Miller, K.J., "Requirements of a New Multiaxial Fatigue Testing Facility," Multiaxial Fatigue, ASTM STP 853, ed. K.J. Miller and M.W. Brown, 11-23 (1985).

3. Pascoe, K.J. and de Villiers, J.W.R., "Low-Cycle Fatigue of Steels Under Biaxial Straining," J. Strain Anal., **2**, *117-126 (1967).*

4. Parsons, M.W. and Pascoe, K.J., "Development of a Biaxial Fatigue Testing Rig," J. Strain Anal., **10**, *1-9 (1975).*

5. Shiratori, E. and Ikegami, K., "A New Biaxial Tensile Testing Machine With Flat Specimen," Bul. Tokyo Inst. Tech., **82**, *105-118 (1967).*

6. Shimada, H., Shimizu, K., Obata, M., Chikugo, K. and Chiba, M., "A New Biaxial Testing Machine for the Flat Specimen and a Fundamental Study on the Shape of Specimen," Tech. Rep., Tohoku Univ., **41**, *351-369 (1976).*

7. Hopper, C.D. and Miller, K.J., "Fatigue Crack Propagation in Biaxial Stress Fields," J. Strain Anal., **12**, *23-28 (1977).*

8. Daniel, I.M., "Behavior of Graphite/Epoxy Plates With Holes Under Biaxial Loading," EXPERIMENTAL MECHANICS, **20**, *1-8 (1980).*

9. Charvat, I.M.H. and Garrett, G.G., "The Development of a Closed-Loop, Servo-Hydraulic Test System for Direct Stress Monotonic and Cyclic Crack Propagation Studies Under Biaxial Loading," J. Test. Eval., **8**, *9-17 (1980).*

10. Liu, A.F. and Yamane, J.R., "Crack Growth Under Equibiaxial Tension," Res. Mech., **5**, *1-11 (1982).*

11. Jones, D.L., Poulose, P.K. and Liebowitz, H., "The Effects of Biaxial Loading on the Fracture Characteristics of Several Engineering Materials," Eng. Fract. Mech., **24**, *187-205 (1986).*

12. Bert, C.W., Mayberry, B.L. and Ray, J.D., "Behavior of Fiber-Reinforced Plastic Laminates Under Biaxial Loading," ASTM STP 460, 362-380 (1969).

13. Ferron, G. and Makinde, A., "Design and Development of a Biaxial Strength Testing Device," J. Test. Eval., **16**, *253-256 (1988).*

14. Johnson, A.E. and Khan, B., "A Biaxial-Stressing Creep Machine and Extensometer," Proc. Inst. Mech. Eng., **180A**, *318-323 (1965-66).*

15. Hayhurst, D.R., "A Biaxial-Tension Creep-Rupture Testing Machine," J. Strain Anal., **8**, *119-123 (1973).*

16. Kelly, D.A., "Problems in Creep Testing Under Biaxial Stress Systems," J. Strain Anal., **11**, *1-6 (1976).*

17. Fessler, H. and Musson, J.K., "A 30-Ton Biaxial Testing Machine," J. Strain Anal., **4**, *22-26 (1969).*

18. Chaudonneret, M., Gilles, P., Labourdette, R. and Policella, H., "Machine d'essais de traction biaxiale pour essais statiques et dynamiques," La Recherche Aérospatiale, **5**, *299-305 (1977).*

19. Makinde, A., Thibodeau, L., Lefebvre, D., Neale, K.W. and Lahoud, A.E., "Development of a Servohydraulic Machine for Testing Cruciform Specimens," Proc. 1989 SEM Spring Conf. on Exp. Mech., 112-116 (1989).

20. MTS Systems Corporation, Minneapolis, Minnesota, Technical service manuals.

21. Makinde, A., Thibodeau, L., Neale, K.W. and Lefebvre, D., "Design of a Biaxial Extensometer for Measuring Strains in Cruciform Specimens," EXPERIMENTAL MECHANICS, **22** *(2), (1992).*

22. Smith, E.W. and Pascoe, K.J., "The Behaviour of Fatigue Cracks Subject to Applied Biaxial Stress: A Review of Experimental Evidence," Fatigue Eng. Mat. Struct., **6**, *201-224 (1983).*

23. Monch, E. and Galster, D., "A Method for Producing a Defined Uniform Biaxial Tensile Stress Field," Brit. J. Appl. Phys., **14**, *810-812 (1963).*

24. Liu, A.F., Allison, J.E., Dittmer, D.F. and Yamane, J.R., "Effect of Biaxial Stresses on Crack Growth," ASTM STP 677, ed. C.W. Smith, 5-22 (1979).

25. Parsons, M.W. and Pascoe, K.J., "Low-Cycle Fatigue Under Biaxial Stress," Proc. Inst. Mech. Eng., **188**, *657-675 (1975).*

26. Makinde, A., "Mise au point d'un dispositif original de traction biaxiale: Application à l'étude expérimentale de l'écrouissage des metaux sous différents chemins de déformation," PhD Thesis, Université de Poitiers, Poitiers, France (1986).

27. Kreissig, R. and Schindler, J., "Some Experimental Results on Yield Condition in Plane Stress State," Acta Mech., **65**, *169-179 (1986).*

28. Bremand, F. and Lagarde, A., "Optical Method of Strain Measurements: Biaxial Tension Specimen for Birefringent Elastomer," Arch. Mech., **40**, *515-527 (1988).*

29. Box, G.E.P., Hunter, W.G. and Hunter, J.S., Statistics for Experimenters, John Wiley & Sons, New York (1978).

30. Wilson, I.H. and White, D.J., "Cruciform Specimens for Biaxial Fatigue Tests: An Investigation Using Finite Element Analysis and Photoelastic-Coating Techniques," J. Strain Anal., **6**, *27-37 (1971).*

31. Hill, R., "A General Theory of Uniqueness and Stability in Elastic-Plastic Solids," J. Mech. Phys. Solids, **6**, *236-249 (1958).*

32. Hutchinson, J.W., "Finite Strain Analysis of Elastic-Plastic Solids and Structures," Numerical Solution of Non-Linear Structural Problems, ed. R.F. Hartung, ASME, 17-29 (1973).

33. Neglo, K., Chater, E. and Neale, K.W., "Effects of the Shape of a Geometric Defect and of Interactions Between Defects on Limit Strains for Biaxially Stretched Sheets," Int. J. Mech. Sci., **29**, *807-820 (1987).*